

Experimental Investigation of Drain Noise in High Electron Mobility Transistors: Thermal and Hot Electron Noise

Bekari Gabritchidze¹, Kieran A. Cleary¹, Anthony C. Readhead¹, Austin J. Minnich²

Abstract—We report the on-wafer characterization of S -parameters and microwave noise temperature (T_{50}) of discrete metamorphic InGaAs high electron mobility transistors (mHEMTs) at 40 K and 300 K and over a range of drain-source voltages (V_{DS}). From these data, we extract a small-signal model and the drain (output) noise current power spectral density (S_{id}) at each bias and temperature. This procedure enables S_{id} to be obtained while accounting for the variation of small-signal model, noise impedance match, and other parameters under the various conditions. We find that the thermal noise associated with the channel conductance can only account for a portion of the measured output noise. Considering the variation of output noise with physical temperature and bias and prior studies of microwave noise in quantum wells, we hypothesize that a hot electron noise source based on real-space transfer of electrons from the channel to the barrier could account for the remaining portion of S_{id} . We suggest further studies to gain insights into the physical mechanisms. Finally, we calculate that the minimum HEMT noise temperature could be reduced by up to $\sim 50\%$ and $\sim 30\%$ at cryogenic temperature and room temperature, respectively, if the hot electron noise could be suppressed.

Index Terms—High electron mobility transistors, cryogenic electronics, microwave noise, low-noise amplifiers, drain temperature, real-space transfer

I. INTRODUCTION

HIGH electron mobility transistors are widely employed in microwave amplifiers due to their low noise characteristics [1], [2], [3], [4], [5]. While significant improvements have been made in their noise and frequency performance in past decades [6], [7], [8], [9], [10], achieving further improvements requires a physics-based understanding of the origin of microwave noise in low noise HEMTs which is lacking. Presently, noise in HEMTs is interpreted with the Pospieszalski model [11] in which noise is described using two uncorrelated noise generators at the input (S_{vg}) and output (S_{id}). The input noise generator, S_{vg} , is described using a noise temperature T_g which is assigned to the intrinsic gate resistance, and this noise temperature is generally accepted

to be the physical temperature of the gate resistance [12], [13]. This gate resistance thermal noise is significantly larger than the induced gate noise for frequencies far below the cut-off frequency [14]. The output noise generator, S_{id} , is described by assigning a noise temperature, T_d , to the intrinsic output conductance g_{ds} . T_d is generally taken as a fitting parameter. Despite the utility of the model in interpreting noise measurements on HEMTs, it is unable to provide insight into the physical origin of the output noise.

Other works have proposed various mechanisms; for instance, thermal noise has been suggested as the origin of channel noise in field effect transistors (FETs) [15] such as HEMTs [16], [17] and MOSFETs [18], [19]. A recent work attributed drain noise to suppressed shot noise [20] while others to thermal and suppressed shot noise [21].

Another theory attributes drain noise to microwave partition noise arising from real-space transfer (RST) [22], a process that has been investigated in early studies of transport and noise in quantum wells [23], [24], [25], [26], [27]. In this mechanism, electrons are heated by the electric field under the gate to physical temperatures exceeding 1000 K, a temperature sufficiently high that some electrons may thermionically emit out of the channel into the barrier. Because the barrier mobility is substantially less than that of the channel, two dissimilar conduction pathways exist from source to drain, creating partition noise [28] at the HEMT output. However, which of these mechanisms is the actual origin of drain noise in low-noise HEMTs remains under investigation.

In this paper, we performed on-wafer S -parameter and microwave noise measurements (T_{50}) of discrete metamorphic InGaAs mHEMTs at 40 K and 300 K and various V_{DS} using a cryogenic probe station. At each temperature and bias we extracted a small-signal model (SSM) and noise parameters from the S -parameter and T_{50} measurements, allowing the output current noise PSD (S_{id}) to be extracted while accounting for changes in small-signal parameters and optimal noise impedance at each condition. We find that the variation of S_{id} with physical temperature is inconsistent with suppressed shot noise as the sole noise source, and further, that S_{id} cannot be explained only by channel thermal noise. Considering the conclusions of prior studies of microwave noise in quantum wells, we propose that the additional hot-electron noise is due to real-space transfer of electrons from the channel to the barrier, and we suggest how this hypothesis could be tested in future studies. Finally, we compute that the minimum noise temperature could be decreased by 50% and 30% at cryogenic

This work was supported by the National Science Foundation under Grant No. 1911220. (Corresponding author: A. J. Minnich)

B. Gabritchidze is with the Division of Physics, Mathematics and Astronomy, California Institute of Technology, Pasadena, CA, 91125, and also with the Department of Physics, University of Crete, GR-70013 Heraklion, Greece (bekari@caltech.edu)

K. A. Cleary and A. C. Readhead are with the Division of Physics, Mathematics and Astronomy, California Institute of Technology, Pasadena, CA, 91125. (kcleary@astro.caltech.edu, acr@astro.caltech.edu)

A. J. Minnich is with Division of Engineering and Applied Science, California Institute of Technology, Pasadena, CA, 91125 (aminnich@caltech.edu)

and room temperature, respectively, if the hot-electron noise were suppressed.

This paper is organized as follows. A brief description of the experimental set up and the modeling is presented in Section II. The S -parameter and microwave noise characterization and the extracted drain noise current PSD are presented in Section III. The contributions of thermal noise to drain noise is presented in Section IV, followed by a discussion of the hot electron part of drain noise and a possible explanation based on RST in Section V. Finally, we provide a summary of the paper in Section VI.

II. ON-WAFER CRYOGENIC CHARACTERIZATION AND MODELING

The S -parameters and the microwave noise temperature of metamorphic InGaAs mHEMTs (OMMIC, D007IH, 4F50, gate length $L_g = 70$ nm) were measured using a cryogenic probe station (CPS) [29]. Details of the measurement procedure and the experimental set-up were described earlier [30]. In brief, the S -parameter measurements were carried out in the frequency range 1 – 18 GHz using a vector network analyzer (VNA, Rhode&Schwartz ZVA50). The system was calibrated by transferring the measurement plane from the VNA to the tips of the wafer probes (GGB industries, 40A-GSG-100-DP) by through-reflect-match (TRM) calibration on a CS-5 calibration substrate (GGB Industries) at each physical temperature.

The microwave noise temperature was measured using the Y-factor method with a cold attenuator [30], [31] at a generator impedance of 50Ω . The CPS was configured for noise measurements from 2–18 GHz, however, the measurement bandwidth was chosen from 5–15 GHz to minimize RF probe–pad contact time and avoid RF pad damage due to chuck vibrations. A 10 dB cryogenic and a room temperature attenuator (Quantum Microwave) were inserted between the noise source (Keysight, N4002A) and the device under test (DUT). The room-temperature attenuator was connected directly to the noise source (NS) to reduce the change in output reflections from the ‘on’ to ‘off’ state of the NS, while the cryogenic attenuator was connected to the RF input probe contacting the input of the DUT and served as a cold load. After the DUT, a cryogenic amplifier (Cosmic Microwave, CIT1-18) was used after the output probe within the probe station, and a combination of mixer, oscillator, filters, amplifiers and a power sensor were used outside the probe station to further process and measure the incident noise power. A detailed schematic was presented in [30].

An analysis indicated that the uncertainty in noise temperature arose primarily from uncertainty in the input loss. These losses consist of stainless steel coaxial cable, cryogenic 10 dB attenuator, cryogenic bias tee, and the input RF probe. These losses were characterized in a separate cryogenic dewar at each temperature for which noise measurements were performed. The insertion loss of the input RF probe was measured at room temperature by measuring the return loss with the probe tips open, but it could not be measured at cryogenic temperatures. Therefore, an uncertainty of 0.1 dB on the input loss was

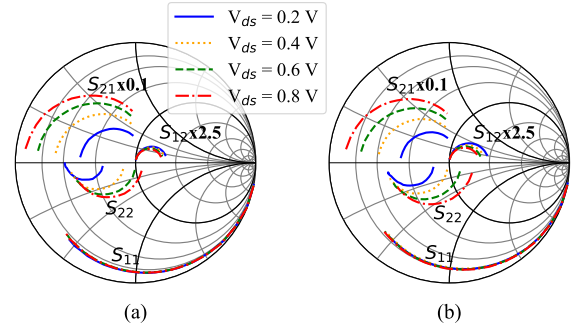


Fig. 1: Measured S -parameters versus frequency over 1 – 18 GHz at various V_{DS} and physical temperatures of 40 K (a) and 300 K (b).

assumed for the RF probe to account for any changes in its insertion loss as T_{ph} is decreased from 300 K to 40 K. Its temperature was assumed to be that of the cryogenic bias tee connected to the RF probe. Based on an uncertainty of 0.1 dB in the input loss, an absolute uncertainty in T_{50} of $\sim 20\%$ at $T_{ph} = 40$ K and $\sim 15\%$ at $T_{ph} = 300$ K was determined. The repeatability of the T_{50} measurements was $\lesssim 0.5$ K at $T_{ph} = 40$ K and ~ 1 K at $T_{ph} = 300$ K.

From the S -parameter and T_{50} measurements, a 15-element small-signal model (SSM) was developed. First, the parasitics were extracted through cold-FET measurements following [32], [33], [34], [35], [36]. Once the parasitics were determined and de-embedded, the intrinsic parameters were evaluated by direct extraction and optimization of the intrinsic parameters. Simulated annealing and quasi-Newton optimization, available in Advanced Design System (ADS, Keysight), were used to minimize a least-square error function following [30]. After the optimization, the intrinsic parameters were further fine tuned to improve the agreement between the measured and simulated S -parameters. Temperature independence of the extracted parasitic capacitances and inductances was assumed based on [37], [35], and the 300 K values were used at all T_{ph} . The parasitic resistances (R_g, R_s, R_d) have been reported to vary $\sim 50\%$ as T_{ph} is decreased from 300 K to 40 K [35]; however, these resistances are difficult to measure at cryogenic temperatures. We estimated the effect of decreasing parasitic resistances by 50% in the 40 K SSM on the SSM parameters and S_{id} and found that this change altered g_m and R_{ds} by $\sim 5\%$ and S_{id} by $\sim 6\%$. Therefore, we neglected the temperature dependence of the parasitic resistances. Additionally, the parasitics are bias-independent [35], so at a given T_{ph} the observed V_{DS} dependent trends are not affected by the assumption of constant parasitic resistance. However, the absolute values of minimum noise temperature (T_{min}) with V_{DS} at $T_{ph} = 40$ K are overestimated by $\sim 10\%$ at 6 GHz when the parasitic resistance at 300 K is used for all temperatures. SSM parameter extraction was carried out for $V_{DS} \geq 0.1$ V, as in this voltage range the gain exceeded 10 dB and the SSM yielded an average normalized error function [38] of $\sim 2\%$.

Under these assumptions, a noise model based on the

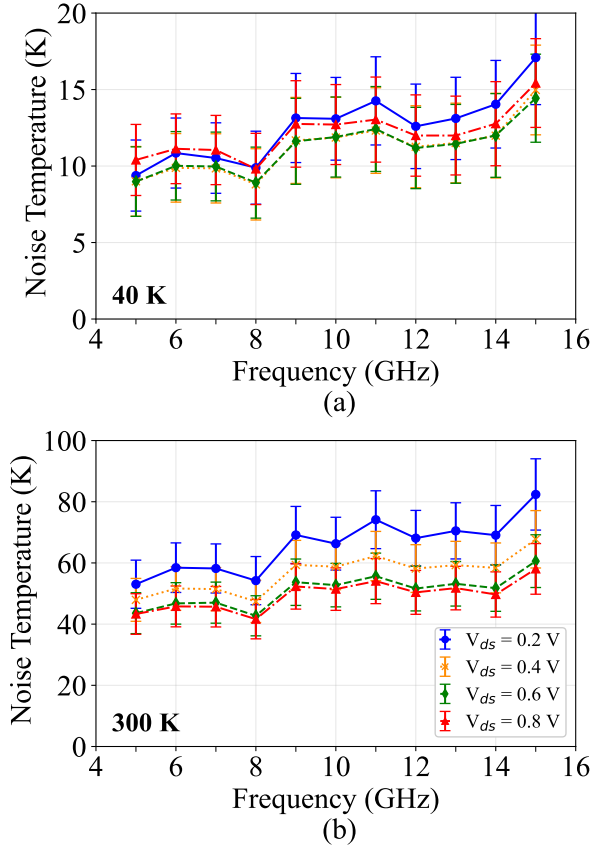


Fig. 2: Measured T_{50} versus frequency at various V_{DS} and physical temperature of 40 K (a) and 300 K (b). The V_{GS} remained constant at all V_{DS} with $V_{GS} = -136$ mV and $V_{GS} = -226$ mV at 40 K and 300 K, respectively.

Pospieszalski model [11] was obtained by fitting the measured and modeled T_{50} using S_{id} as a fitting parameter. The uncertainties in S_{id} reported as the error bars in the subsequent figures include the uncertainties in access resistances, g_{ds} and T_{50} measurements; however, the total uncertainty in S_{id} is dominated by the uncertainty in our T_{50} measurements.

III. RESULTS

Fig. 1 shows the measured S -parameters at various V_{DS} ranging from 0.2 – 0.8 V and physical temperatures of 40 K and 300 K. At a given T_{ph} , S_{21} and S_{22} exhibit the largest variation with V_{DS} , while S_{12} and S_{11} show smaller but observable dependence. In Fig. 2, T_{50} versus frequency is shown for various V_{DS} and the two physical temperatures. In both the S -parameter and noise measurements, the gate voltage (V_{GS}) was kept constant at $V_{GS} = -136$ mV at $T_{ph} = 40$ K, and $V_{GS} = -226$ mV at $T_{ph} = 300$ K, for all V_{DS} . These V_{GS} were selected so that $I_{DS} = 20$ mA at $V_{DS} = 0.8$ V and a given T_{ph} . At a given V_{GS} and T_{ph} , the threshold voltage (V_{th}) varied with V_{DS} from -0.23 V to -0.28 V at 40 K and -0.31 V to -0.38 V at 300 K. The V_{th} at each temperature was calculated from the $I_{DS} - V_{GS}$ curves following [39]. V_{DS} was varied from 0.1 V to 1.0 V; V_{DS} was restricted to ≤ 1.0 V so that gate leakage currents (I_G) were $I_G \lesssim 20$

$\mu\text{A}/\text{mm}$ at $T_{ph} = 300$ K, leading to negligible contribution from shot noise [40]. The lowest T_{ph} was limited to 40 K to avoid cryogenic self-heating effects [41], [42], [43].

From these measurements, a noise model was developed which permits the extraction of S_{id} at each bias and temperature using the measured T_{50} and S -parameters while accounting for mismatch between 50Ω and optimum noise impedance. Following the CMOS and MOSFET noise literature [44], [45], [46], [47] we plot S_{id} versus V_{DS} at 40 K and 300 K in Figs. 3a and 3b, respectively. At 40 K, the S_{id} follows a linear trend at low $V_{DS} \lesssim 0.6$ V and rises rapidly at higher voltages. A similar trend is found at 300 K.

Regarding the rapid increase in S_{id} at high voltages, we note that no indications of non-ideal effects like impact ionization were present in the DC characteristics or S -parameters in our devices. The I-V curves (available in [30, Fig. 3]) did not show any kink, while the gate-source current, I_{GS} , remained at values between $-5 \mu\text{A}/\text{mm}$ and $-20 \mu\text{A}/\text{mm}$, far from the bias regime where impact ionization was observed previously in our devices [36, Fig. 6.7]. Additionally, S_{22} remained capacitive for all V_{DS} [48]. However, it has been reported based on Monte Carlo simulations [49] that microwave noise from impact ionization may occur even though it may not be observable in I-V and S -parameters measurements. Therefore, it is possible that the rapid increase in S_{id} above 0.8 V is due to impact ionization.

The variation of T_d with T_{ph} for the present devices has been previously reported in [30]. Here, we use those data and the present measurements to obtain S_{id} versus T_{ph} at constant $V_{DS} = 0.6$ V and $I_{DS} = 10$ mA in Fig. 4. A dependence of S_{id} on T_{ph} is observed. This observation contradicts the predictions of suppressed shot noise theory. According to this theory, if I_{DS} is kept constant with physical temperature, then the output noise current S_{id} is predicted to be temperature-independent. [20], [50], [51] This prediction is inconsistent with the measured temperature dependence of the output noise current in Fig. 5a. This conclusion agrees with the findings of [52], [30], [37], [53]. This finding indicates that suppressed shot noise cannot be the sole mechanism contributing to drain noise.

IV. CONTRIBUTION OF CHANNEL THERMAL NOISE TO OUTPUT NOISE

We now discuss what physical mechanisms could account for the observed trends of drain noise PSD. Drain noise in HEMTs, like other field effect transistors, is expected to originate at least in part from thermal noise of the channel conductance. The relevant portion of the channel of interest for its noise contribution is that under the gate recess, as the other access resistances have been already taken into account in the SSM. The thermal noise of the channel subject to gate and drain biases is given by $S_{id,th} = 4k_B g_{dso} T_{ph} \gamma$, where, k_B is the Boltzmann constant, g_{dso} is the channel conductance at $V_{DS} = 0$ V, and γ is a factor that accounts for the variation in carrier density along the channel due to the combined effect of the gate-source and drain-source potentials [16], [45], [47]. In the linear region, $\gamma = 1$, while in saturation

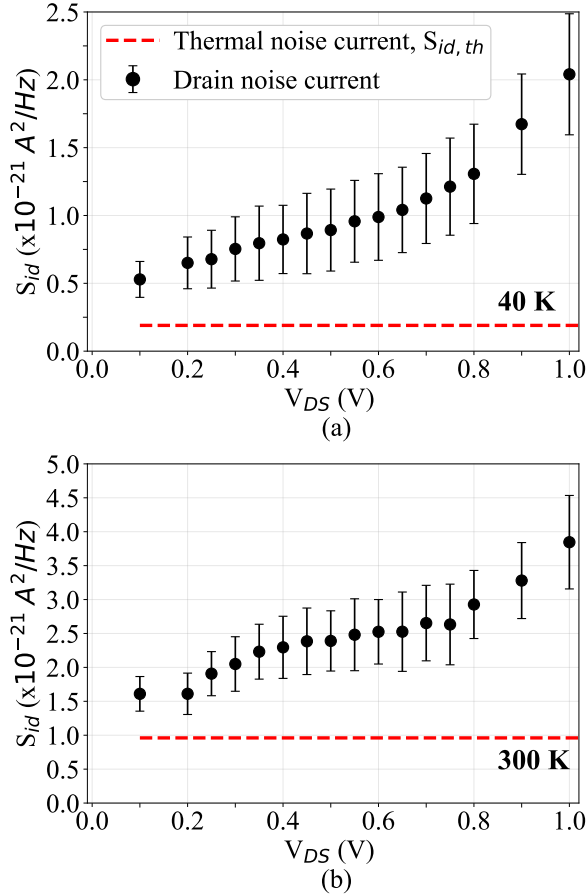


Fig. 3: Extracted SSM S_{id} (black circles) and computed channel thermal noise PSD S_{th} (red dashed line) versus V_{DS} at 40 K (a) and 300 K (b). The gate voltage, V_{GS} was -136 mV at $T_{ph} = 40$ K, and -226 mV at $T_{ph} = 300$ K.

its values depend on the channel length; in the long-channel limit $\gamma = 2/3$ using the gradual-channel approximation, while in short-channel devices γ varies between 1 and 2 due to short-channel effects such as velocity saturation and channel-length modulation [54], [45], [55]. $S_{id,th}$ is also affected by high-field effects such as non-equilibrium carrier heating, meaning that electrons are heated above the lattice temperature. Although the higher electron temperature increases S_{id} , the high-field conductance is generally lower than the low-field value due to the decrease in mobility with increasing field. In addition, the carrier density in the pinch-off region is at least an order of magnitude lower than that of the unperturbed channel [5].

Considering these competing trends, various studies have concluded that the noise from the pinch-off region is negligible [45], [56], [57]. This conclusion is compatible with experimental measurements of microwave noise in InGaAs quantum wells, which show that the current PSD decreases with increasing field [25, Fig. 16.7]. Therefore, an overestimate for the channel thermal noise may be obtained by taking $S_{id,th} = 4k_B g_{dso} T_{ph}$, neglecting the decrease in noise associated with the formation of the pinch-off region at high V_{DS} . g_{dso} is obtained from the slope of the I-V characteristics at $V_{DS} = 0$ V.

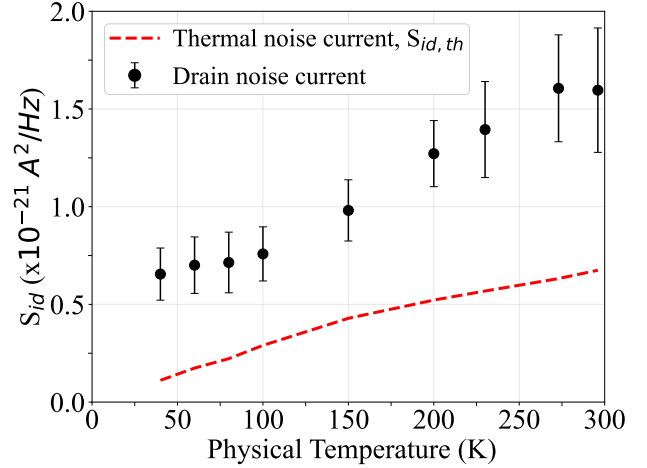


Fig. 4: Extracted SSM drain noise PSD S_{id} (black circles) versus physical temperature T_{ph} and computed thermal noise PSD $S_{id,th}$ (red dashed line) at constant $V_{DS} = 0.6$ V and $I_{DS} = 10$ mA (computed from data reported in [30]).

In Figs. 3a and 3b, the computed $S_{id,th}$ are shown at 40 K and 300 K, respectively. The measured S_{id} exceeds the channel thermal noise magnitude, corresponding to γ values of $\sim 3-6$ at 40 K and $\sim 2-3$ at 300 K. However, theories of channel thermal noise including short-channel effects generally predict $\gamma \lesssim 1.5$. [45], [54] Fig. 4 shows the T_{ph} dependence of S_{id} and $S_{id,th}$ at constant $V_{DS} = 0.6$ V and $I_{DS} = 10$ mA. For the calculation of $S_{id,th}$, g_{dso} was derived from the I-V curves at each T_{ph} and was corrected for the access resistances following [47], [58]. While $S_{id,th}$ qualitatively accounts for the temperature-dependence of S_{id} , the measured trend plateaus below 100 K while $S_{id,th}$ tends to zero with decreasing temperature. Additionally, the magnitude of $S_{id,th}$ is $\sim 50-70\%$ lower than the measured values. Considering the totality of the observations, the analysis suggests that another mechanism beyond channel thermal noise contributes to drain noise in HEMTs.

V. DISCUSSION

We now discuss potential physical origins of the additional drain noise source. Suppressed shot noise can arise if electrons propagate quasi-ballistically in the channel. However, ultrafast optical studies have found that photoexcited electrons in quantum wells thermalize within 200 fs, implying an electron-electron collision time on the order of 10 fs. [59, Sec. 4C3b]. Considering a drift velocity of $\sim 5 \times 10^7$ cm s⁻¹ [60], these values yield a mean free path of around 5-10 nm. This value is much shorter the gate length or source-drain separation of even highly-scaled HEMTs, implying that suppressed shot noise is not likely to be a relevant noise mechanism in HEMTs.

Another theory for drain noise based on real-space transfer of hot electrons from the channel to barrier films was developed following the conclusions of prior studies of microwave noise in quantum wells [22]. Specifically, in earlier experimental works the microwave noise temperature was found to be affected by alterations to the quantum well potential

even with the channel alloy composition held constant, suggesting that the heterojunction potential confining the channel electrons played a role in the noise mechanism [27], [26]. This observation is compatible with the real-space transfer mechanism in which hot electrons thermionically emit over the confining barrier potential to create partition noise. [22] derived an expression for S_{id} in which noise arises due to RST; however, this work did not consider the contribution of channel thermal noise.

Here, we suggest that drain noise could be attributed to a combination of channel thermal noise and RST: $S_{id} = S_{th,id} + S_{RST}$. The S_{RST} is defined in [22, Eq. (3)] and depends exponentially on the peak electron temperature, the conduction band discontinuity (ΔE_c) at the channel/barrier heterojunction and the overdrive voltage defined as $V_{ov} = V_{gs} - V_{th}$, where V_{th} the threshold voltage. In [22], the peak electron temperature was assumed to vary linearly with the physical temperature. However, Monte Carlo studies [61] and the weak temperature-dependence of high-field velocity characteristics in many semiconductors indicate that the peak electron temperature in HEMTs should exhibit a weak dependence on lattice temperature. In this case, RST noise would be predicted to exhibit only a weak dependence on physical temperature as well. This conclusion differs from that originally reported in [22].

Qualitatively, the trend of S_{id} versus T_{ph} in Fig. 4 can be explained if the thermal noise is responsible for the primary T_{ph} dependence, with another mechanism with weaker temperature dependence accounting for the overall trend and magnitude. Using the numerical values given in [22] and assuming $V_{ov} = 43$ mV from the measurements in this work, we compute $S_{id,RST} \sim 3 \times 10^{-22}$ A²/Hz over the range of temperatures studied, which is of the right order of magnitude to explain the discrepancy. However, we caution that this estimate is only valid to within a factor of 2-3 owing to uncertainties in the parameters described in [22].

The role of RST in drain noise could be further confirmed by examining how the microwave noise temperature trends with bias and temperature are affected by changes in quantum confinement of channel electrons, for instance by altering the conduction band offset while not varying the channel composition so as to avoid confounding effects from impact ionization, for example. This modification can be accomplished by increasing the Al composition of the barrier [62]. Strained-barrier HEMTs with Al composition of over 55% have been reported [63], and so such a study appears feasible.

Finally, we use our noise model to estimate the magnitude of improvement in T_{min} if the channel noise were only due to thermal noise. In Ref. 5, we plot the extracted T_{min} , obtained from the noise model using S-parameter and T_{50} data versus V_{DS} at T_{ph} of 40 K and 300 K, and frequency of 6 GHz. In this plot, we also show the predicted trend of T_{min} if drain noise was due solely to channel thermal noise. We observe that the minimum T_{min} could be improved by $\sim 50\%$ and $\sim 30\%$ at 40 K and 300 K, respectively. This result implies that if the hot-electron noise observed in S_{id} originates from RST, then significant improvements in cryogenic and room temperature noise performance may

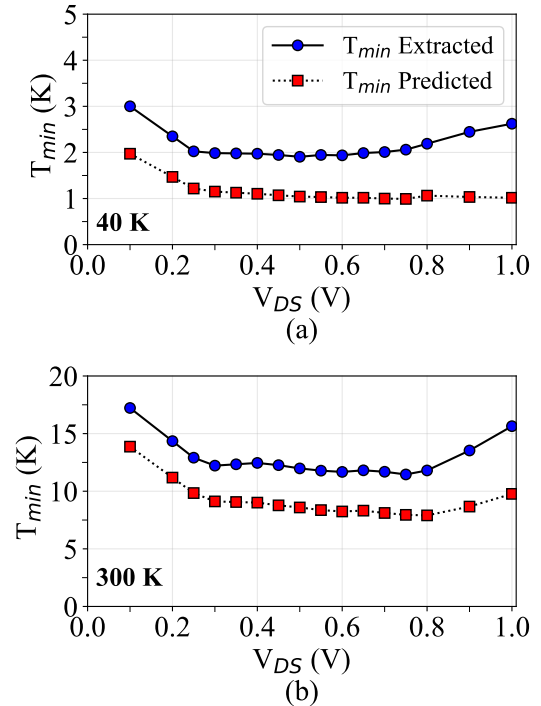


Fig. 5: Extracted T_{min} [30] and predicted T_{min} with only channel thermal noise versus V_{DS} at 40 K (a) and 300 K (b) and constant $V_{GS} = -136$ mV and $V_{GS} = -226$ mV, respectively. The predicted T_{min} is obtained by replacing by setting $S_{id} = S_{th}$ in the noise model. All the above data are at the frequency of 6 GHz. The V_{GS} in (a) and (b) were selected so that at both physical temperatures, $V_{DS} = 0.8$ V and $I_{ds} = 20$ mA.

be possible by engineering the quantum well for improved quantum confinement.

VI. CONCLUSION

We have characterized the S -parameters and the microwave noise temperature of InGaAs mHEMTs at 40 K and 300 K and various V_{DS} . The extracted drain noise is found to exceed that expected from channel thermal noise by a factor of ~ 2 -6, suggesting that an additional mechanism contributes to drain noise. Based on prior studies of microwave noise in quantum wells, we hypothesize that this noise mechanism is real-space transfer noise. We suggest approaches to further test this hypothesis. Finally, we compute that improvements in minimum cryogenic noise temperature of up to 50% can be achieved if the hot-electron noise is suppressed.

ACKNOWLEDGMENTS

The authors thank Jan Grahn, Pekka Kangaslahti, Jacob Kooi, Junjie Li, Jun Shi and Sander Weinreb for useful discussions.

REFERENCES

- [1] T. Mimura, "The early history of the high electron mobility transistor (HEMT)," *IEEE Trans. Microw. Theory Tech.*, vol. 50, no. 3, pp. 780–782, 2002.

- [2] P. E. Longhi, L. Pace, S. Colangeli, W. Ciccognani, and E. Limiti, "Technologies, design, and applications of low-noise amplifiers at millimetre-wave: State-of-the-art and perspectives," *J. Electron.*, vol. 8, no. 11, p. 1222, 2019.
- [3] A. Reinhard, "Ultra-low noise InP HEMTs for cryogenic applications - fabrication, modeling and characterization," phdthesis, ETH ZURICH, 2013.
- [4] E. Bryerton, M. Morgan, and M. Pospieszalski, "Ultra low noise cryogenic amplifiers for radio astronomy," in *IEEE Radio Wireless Symp.*, Jan. 2013, pp. 358–360.
- [5] F. Schwierz and J. J. Liou, *Modern Microwave Transistors: Theory, Design, and Performance*, 1st ed. NY, USA: Wiley-Intersci. Ser., 2002.
- [6] E. Cha, N. Wadefalk, G. Moschetti, A. Pourkabirian, J. Stenarson, and J. Grahn, "A 300- μ W Cryogenic HEMT LNA for Quantum Computing," in *IEEE MTT-S Int. Microw. Symp.*, Aug. 2020, pp. 358–360.
- [7] E. Cha, N. Wadefalk, S.-N. Nilsson, J. Schlee, G. Moschetti, A. Pourkabirian, S. Tuzi, and J. Grahn, "0.314 and 1628 ghz Wide-Bandwidth Cryogenic MMIC Low-Noise Amplifiers," *IEEE Trans. Microw. Theory Tech.*, vol. 66, no. 11, pp. 4860–4869, 2018.
- [8] W. R. Deal, K. Leong, V. Radisic, S. Sarkozy, B. Gorospe, J. Lee, P. H. Liu, W. Yoshida, J. Zhou, M. Lange, R. Lai, and X. B. Mei, "Low noise amplification at 0.67 thz using 30 nm inp hemts," *IEEE Microw. Wirel. Compon. Lett.*, vol. 21, no. 7, pp. 368–370, 2011.
- [9] F. Thome, F. Schfer, S. Trk, P. Yagoubov, and A. Leuther, "A 67-116-GHz Cryogenic Low-Noise Amplifier in a 50-nm InGaAs Metamorphic HEMT Technology," *IEEE Microw. Wirel. Compon. Lett.*, pp. 1–4, 2021.
- [10] D. Cuadrado-Calle, D. George, G. A. Fuller, K. Cleary, L. Samoska, P. Kangaslahti, J. W. Kooi, M. Sorja, M. Varonen, R. Lai, and X. Mei, "Broadband MMIC LNAs for ALMA Band 2+3 With Noise Temperature Below 28 K," *IEEE Trans. Microw. Theory Tech.*, vol. 65, no. 5, pp. 1589–1597, May 2017.
- [11] M. Pospieszalski, "Modeling of noise parameters of mesfets and modfets and their frequency and temperature dependence," *IEEE Trans. Microw. Theory Tech.*, vol. 37, no. 9, pp. 1340–1350, 1989.
- [12] M. W. Pospieszalski, "On the dependence of FET noise model parameters on ambient temperature," in *IEEE Radio Wireless Symp.*, 2017, pp. 159–161.
- [13] M. Pospieszalski, "Interpreting transistor noise," in *IEEE Microw. Mag.*, Oct. 2010, pp. 61–69 vol.11.
- [14] P. Heymann and M. Rudolph, *A Guide to Noise in Microwave Circuits: Devices, Circuits and Measurement*, 1st ed. Wiley-IEEE Press, 2021.
- [15] A. V. Der Ziel, "Thermal noise in field-effect transistors," *Proc.IRE*, vol. 50, no. 8, pp. 1808–1812, 1962.
- [16] A. van der Ziel and E. N. Wu, "Thermal noise in high electron mobility transistors," *Solid-State Electron.*, vol. 26, no. 5, pp. 383–384, 1983.
- [17] A. van der Ziel, "Thermal noise in the hot electron regime in fet's," *IEEE Trans. Electron Devices*, vol. 18, no. 10, pp. 977–977, 1971.
- [18] J. Paasschens, A. Scholten, and R. van Langevelde, "Generalizations of the klaassen-prins equation for calculating the noise of semiconductor devices," *IEEE Trans. Electron Devices*, vol. 52, no. 11, pp. 2463–2472, 2005.
- [19] A. Roy, C. Enz, and J.-M. Sallese, "Noise modeling methodologies in the presence of mobility degradation and their equivalence," *IEEE Trans. Electron Devices*, vol. 53, no. 2, pp. 348–355, 2006.
- [20] M. W. Pospieszalski, "On the limits of noise performance of field effect transistors," in *IEEE MTT-S Int. Microw. Symp.*, 2017, pp. 1953–1956.
- [21] K. Ohmori and S. Amakawa, "Direct white noise characterization of short-channel mosfets," *IEEE Trans. Electron Devices*, vol. 68, no. 4, pp. 1478–1482, 2021.
- [22] I. Esho, A. Y. Choi, and A. J. Minnich, "Theory of drain noise in high electron mobility transistors based on real-space transfer," *J. Appl. Phys.*, vol. 131, no. 8, p. 085111, Feb. 2022.
- [23] A. Matulionis, V. Aninkevicius, J. Berntgen, D. Gasquet, J. Liberis, and I. Matulionis, "QW-shape-dependent hot-electron velocity fluctuations in InGaAs-based heterostructures," *Phys. Status Solidi*, vol. 204, no. 1, pp. 453–455, 1997.
- [24] A. Matulionis, V. Aninkevicius, and J. Liberis, "Hot-electron velocity fluctuations in two-dimensional electron gas channels," *Microelectron. Reliab.*, vol. 40, no. 11, pp. 1803–1814, 2000.
- [25] H. Hartnagel, R. Katilius, and A. Matulionis, *Microwave Noise in Semiconductor Devices*, 1st ed. NY, USA: Wiley-Intersci. Ser., 2001.
- [26] V. Aninkevicius, V. Bareikis, R. Katilius, P. S. Kopev, M. R. Leys, J. Liberis, and A. Matulionis, "Hot-electron noise and diffusion in AlGaAs/GaAs," *Semicond. Sci. Technol.*, vol. 9, no. 5S, pp. 576–579, may 1994.
- [27] V. Aninkevicius, V. Bareikis, J. Liberis, A. Matulionis, and P. Sakalas, "Comparative analysis of microwave noise in GaAs and AlGaAs/GaAs channels," *Solid-state electron.*, vol. 36, no. 9, pp. 1339–1343, sep 1993.
- [28] A. Ambrozy, *Electronic Noise*. McGraw-Hill Col., 1983.
- [29] D. Russell, K. Cleary, and R. Reeves, "Cryogenic probe station for on-wafer characterization of electrical devices," *Rev. Sci. Instrum.*, vol. 83, no. 4, p. 044703, 2012.
- [30] B. Gabritchidze, K. Cleary, J. Kooi, I. Esho, A. C. Readhead, and A. J. Minnich, "Experimental characterization of temperature-dependent microwave noise of discrete hemts: Drain noise and real-space transfer," in *IEEE MTT-S Int. Microw. Symp. Dig.*, 2022, pp. 615–618.
- [31] J. Fernandez, "A Noise Temperature Measurement System Using a Cryogenic Attenuator," *TMO Prog. Rep.*, no. 42, p. 135, 1998.
- [32] G. Dambrine, A. Cappy, F. Heliore, and E. Playez, "A new method for determining the fet small-signal equivalent circuit," *IEEE Trans. Microw. Theory Tech.*, vol. 36, no. 7, pp. 1151–1159, 1988.
- [33] M. Berroth and R. Bosch, "Broad-band determination of the fet small-signal equivalent circuit," *IEEE Trans. Microw. Theory Tech.*, vol. 38, no. 7, pp. 891–895, 1990.
- [34] P. Hower and N. Bechtel, "Current saturation and small-signal characteristics of GaAs field-effect transistors," *IEEE Trans. Electron Devices*, vol. 20, no. 3, pp. 213–220, 1973.
- [35] A. R. Alt and C. R. Bolognesi, "(inp) hemt small-signal equivalent-circuit extraction as a function of temperature," *IEEE Trans. Microw. Theory Tech.*, vol. 63, no. 9, pp. 2751–2755, 2015.
- [36] A. H. Akgiray, "New Technologies Driving Decade-Bandwidth Radio Astronomy: Quad-ridged Flared Horn and Compound-Semiconductor LNAs," Ph.D. dissertation, Cal. Inst. of Tech., Pasadena, CA, USA, 2013.
- [37] F. Heinz, F. Thome, D. Schwantuschke, A. Leuther, and O. Ambacher, "A Scalable Small-Signal and Noise Model for High-Electron-Mobility Transistors Working Down to Cryogenic Temperatures," *IEEE Trans. Microw. Theory Tech.*, vol. 70, no. 2, pp. 1097–1110, Feb. 2022.
- [38] M. Malmkvist, "Optimization of narrow bandgap HEMTs for low-noise and low-power applications," phdthesis, Chalmers Univ. of Technology, 2008.
- [39] D. K. Schroder, *Semiconductor Material and Device Characterization*, 3rd ed. Wiley-IEEE Press, 2015.
- [40] M. W. Pospieszalski, "Extremely low-noise amplification with cryogenic FETs and HFETs: 1970-2004," *IEEE Microw. Mag.*, vol. 6, no. 3, pp. 62–75, 2005.
- [41] J. Schlee, J. Mateos, I. Iiguez-de-la Torre, N. Wadefalk, P. A. Nilsson, J. Grahn, and A. J. Minnich, "Phonon black-body radiation limit for heat dissipation in electronics," *Nat. Mater.*, vol. 14, no. 2, pp. 187–192, 2015.
- [42] A. Y. Choi, I. Esho, B. Gabritchidze, J. Kooi, and A. J. Minnich, "Characterization of self-heating in cryogenic high electron mobility transistors using schottky thermometry," *J. Appl. Phys.*, vol. 130, no. 15, p. Art. No. 155107, 2021.
- [43] A. J. Ardizzi, A. Y. Choi, B. Gabritchidze, J. Kooi, K. A. Cleary, A. C. Readhead, and A. J. Minnich, "Self-heating of cryogenic high electron-mobility transistor amplifiers and the limits of microwave noise performance," *J. Appl. Phys.*, vol. 132, no. 8, p. 084501, 2022.
- [44] G. D. J. Smit, A. J. Scholten, R. M. T. Pijper, R. van Langevelde, L. F. Tiemeijer, and D. B. M. Klaassen, "Experimental demonstration and modeling of excess rf noise in sub-100-nm cmos technologies," *IEEE Electron Device Lett.*, vol. 31, no. 8, pp. 884–886, 2010.
- [45] C.-H. Chen and M. Deen, "Channel noise modeling of deep submicron mosfets," *IEEE Trans. Electron Devices*, vol. 49, no. 8, pp. 1484–1487, 2002.
- [46] V. M. Mahajan, R. P. Jindal, H. Shichijo, S. Martin, F.-C. Hou, and D. Trombley, "Numerical investigation of excess rf channel noise in sub-100 nm mosfets," in *2nd Int. Workshop Electron Devices Semicond. Technol.*, 2009, pp. 1–4.
- [47] G. D. J. Smit, A. J. Scholten, R. M. T. Pijper, L. F. Tiemeijer, R. van der Toorn, and D. B. M. Klaassen, "RF-noise modeling in advanced CMOS technologies," *IEEE Trans. Electron Devices*, vol. 61, no. 2, pp. 245–254, 2014.
- [48] D. C. Ruiz, T. Saranovac, D. Han, O. Ostinelli, and C. Bolognesi, "Impact ionization control in 50 nm low-noise high-speed inp hemts with inas channel insets," in *IEEE Int. Electron Devices Meeting Tech. Dig.*, 2019, pp. 9.3.1–9.3.4.
- [49] B. G. Vasallo, J. Mateos, D. Pardo, and T. Gonzalez, "Kink-effect related noise in short-channel InAlAs/InGaAs high electron mobility transistors," *J. Appl. Phys.*, vol. 95, no. 12, pp. 8271–8274, 06 2004.

- [50] X. Chen, H. Elgabra, C.-H. Chen, J. Baugh, and L. Wei, "Estimation of mosfet channel noise and noise performance of cmos InAs at cryogenic temperatures," in *IEEE ISCAS Int. Symp. Circuits Syst. Dig.*, 2021, pp. 1–5.
- [51] S. K. Kim, A. van der Ziel, and S. T. Liu, "Hot electron noise effects in buried channel MOSFETs," *Solid-State Electron.*, vol. 24, no. 5, pp. 425–428, 1981.
- [52] B. Gabritchidze, K. Cleary, A. Readhead, and A. J. Minnich, "Investigation of drain noise in InP pHEMTs using cryogenic on-wafer characterization," in *IEEE MTT-S Int. Microw. Symp. Dig.*, 2023, pp. 16–19.
- [53] M. Murti, J. Laskar, S. Nuttinck, S. Yoo, A. Raghavan, J. Bergman, J. Bautista, R. Lai, R. Grundbacher, M. Barsky, P. Chin, and P. Liu, "Temperature-dependent small-signal and noise parameter measurements and modeling on InP HEMTs," *IEEE Trans. Microw. Theory Tech.*, vol. 48, no. 12, pp. 2579–2587, 2000.
- [54] A. Scholten, H. Tromp, L. Tiemeijer, R. Van Langevelde, R. Havens, P. De Vreede, R. Roes, P. Woerlee, A. Montree, and D. Klaassen, "Accurate thermal noise model for deep-submicron cmos," in *Int. Electron Devices Meeting Tech. Dig.*, 1999, pp. 155–158.
- [55] C. Jungemann, B. Neinhuis, C. Nguyen, B. Meinerzhagen, R. Dutton, A. Scholten, and L. Tiemeijer, "Hydrodynamic modeling of rf noise in cmos devices," in *IEEE IEDM Int. Electron Dev. Meeting*, 2003, pp. 36.3.1–36.3.4.
- [56] S. N. Ong, K. S. Yeo, K. W. J. Chew, L. H. K. Chan, X. S. Loo, C. C. Boon, and M. A. Do, "Impact of velocity saturation and hot carrier effects on channel thermal noise model of deep sub-micron MOSFETs," *Solid-State Electron.*, vol. 72, pp. 8–11, 2012.
- [57] C. Jungemann and B. Meinerzhagen, "Do hot electrons cause excess noise?" *Solid-State Electron.*, vol. 50, no. 4, pp. 674–679, 2006.
- [58] S. Chou and D. Antoniadis, "Relationship between measured and intrinsic transconductances of fet's," *IEEE Trans. Electron Devices*, vol. 34, no. 2, pp. 448–450, 1987.
- [59] J. Shah, "Hot carriers in quasi-2-d polar semiconductors," *IEEE J. Quantum Electron.*, vol. 22, no. 9, pp. 1728–1743, 1986.
- [60] H. Rodilla, J. Schlee, P.-A. Nilsson, N. Wadefalk, J. Mateos, and J. Grahn, "Cryogenic performance of low-noise InP HEMTs: A monte carlo study," *IEEE Trans. Electron Devices*, vol. 60, no. 5, pp. 1625–1631, may 2013.
- [61] M. Fischetti, "Monte carlo simulation of transport in technologically significant semiconductors of the diamond and zinc-blende structures. i. homogeneous transport," *IEEE Trans. Electron Devices*, vol. 38, no. 3, pp. 634–649, 1991.
- [62] J. Huang, T. Y. Chang, and B. Lalevic, "Measurement of the conductionband discontinuity in pseudomorphic In_xGa_{1-x}As/In_{0.52}Al_{0.48}As heterostructures," *Appl. Phys. Lett.*, vol. 60, no. 6, pp. 733–735, 1992.
- [63] S. Bahl, W. Azzam, and J. del Alamo, "Strained-insulator In_xAl_{1-x}As/In_{0.53}Ga_{0.47}As heterostructure field-effect transistors," *IEEE Trans. Electron Devices*, vol. 38, no. 9, pp. 1986–1992, 1991.